M A T H E M A T I C S D E P A R T M E N T

The Spectral Lagrange Galerkin Method for the Atmospheric Transportation of Pollutants

by

A. Priestley

Numerical Analysis Report 2/89

U N I V E R S I T Y O F R E A D I N G

The Spectral Lagrange Galerkin Method for the Atmospheric Transportation of Pollutants

by

A. Priestley

Numerical Analysis Report 2/89

The work reported here forms part of the research programme of the Reading/Oxford Institute for Computational Fluid Dynamics and has been supported by the S.E.R.C. under grant no GR/E72256.

CONTENTS

1. INTRODUCTION

In recent years there has been much interest and effort aimed at solving advection-dominated diffusion problems. One of the new numerical techniques that has been developed to cope with these problems is the Lagrange-Galerkin method. This method combines the stability properties of the method of characteristics with the accuracy and flexibility of a standard finite element procedure (see Benqué et al (1982), Bercovier & Pironneau (1982), Douglas & Russell (1982), Lesaint (1977), Pironneau (1982), Russell (1980), Süli (1988)). In these papers the unconditional stability and convergence of the Lagrange-Galerkin method has been demonstrated for a wide class of problems as has its practical ability.

Much of the analysis in these papers is based upon the assumption that all the inner products are evaluated exactly, though some study of the influence of quadrature was carried out by Lesaint (1977) and Russell (1982). However, Priestley (1986) and Morton, Priestley & Süli (1988) have shown that many types of quadrature, e.g. Gauss-Legendre, Gauss-Lobatto, Radau and Newton-Cotes, all lead to only a conditionally unstable scheme. Gauss-Legendre quadrature fairs particularly badly in that the instability occurs for small CFL numbers and so cannot be cured by restriction of the time-step. For the other integration rules a severe CFL restriction is incurred which is a major qualification of the unconditional stability of the exactly integrated method. In Priestley et al (1986,1988) a technique is introduced called area-weighting in which all integrations are performed exactly by means of approximating the underlying velocity field. Eastwood & Arter (1986) described a different technique in which they approximated all integrals (including

the evaluation of the mass matrix) by a compound trapezium rule. This results in a careful balance between the anti-diffusive nature of the mass matrix and the smoothing effect of vertex quadrature. However, to approach the accuracy given by the exactly integrated scheme 6,7 or 8 sub-intervals are required, depending upon the problem, which makes the scheme extremely slow when a three-dimensional (or even two-dimensional) problem is being considered.

Meanwhile in meteorological studies the quasi or semi-Lagrangian schemes were being developed. (See Robert (1981,1982), Bates (1985), Staniforth and Temperton (1986), Ritchie (1987) and Temperton and Ritchie (1987) for a flavour of this work.)

In the next section the Lagrange-Galerkin method is derived and the relationship between this method, the EPIC algorithm of Eastwood & Arter (1986) and the semi-Lagrangian method referred to above is discussed. It will be shown that there is room for a great deal of improvement on the handling of the advective forms in the semi-Lagrangian technique.

In Section 3 the Lagrange-Galerkin method is adapted for use with spherical harmonics and a test problem is described, results for which are presented in section 4. Finally in Section 5 a brief summary is given of the work that has been done and possibilities for future work are discussed.

2. THE LAGRANGE GALERKIN METHOD

Consider the Cauchy problem for the scalar, linear advection equation for $u(\underline{x},t)$:

$$u_t + \underline{a}.\ \nabla u = 0\ , \qquad \underline{x} \in \mathbb{R}^d\ ,\ t > 0 \tag{2.1a}$$

$$u(\underline{x},0) = u_0(\underline{x})\ , \tag{2.1b}$$

where u_o belongs to $L^2(\mathbb{R}^d)$ and the velocity field $\underline{a} = \underline{a}(\underline{x},t)$ is incompressible, i.e.

$$\underline{\nabla}\cdot\ \underline{a} = 0 \qquad \forall\ \underline{x},t\ . \tag{2.2}$$

We can define trajectories, $\underline{X}(\underline{x},s;t)$, by

$$\underline{X}(\underline{x},s;s) = \underline{x} \tag{2.3a}$$

$$\frac{d}{dt}\,\underline{X}(\underline{x},s;t) = \underline{a}(\underline{X}(\underline{x},s;t),t) \tag{2.3b}$$

which can be rewritten, if desired, as

$$\underline{X}(\underline{x},s;t) = \underline{x} + \int_s^t \underline{a}(\underline{X}(\underline{x},s;\tau),\tau)d\tau\ . \tag{2.4}$$

Using the obvious notation $t^{n+1} = t^n + \Delta t$, we denote for simplicity the terms $\underline{X}(\underline{y},t^{n+1};t^n)$ and $\underline{X}(\underline{x},t^n;t^{n+1})$ by $\underline{x}$ and $\underline{y}$ respectively.

A unique (absolutely continuous) solution to (2.3) can be guaranteed if it is assumed that $\underline{a}$ belongs to the space $L^1(0,T;\ (W^{1,\infty})^d)$. The relation

$$u(\underline{X}(\cdot,t;t+\tau),\ t+\tau) = u(\cdot,t) \tag{2.5}$$

then gives the solution to (2.1).

The most direct numerical formulation, actually called the direct Lagrange-Galerkin method by Morton and Priestley (1986), for an

approximation

$$U^n(\cdot) = \sum_j U_j^n \phi_j(\cdot) \ , \tag{2.6}$$

at time t^n in terms of finite element basis functions ϕ_j, uses (2.5) directly to obtain U^{n+1} satisfying

$$\langle U^{n+1} \ , \ \phi_i \rangle = \int U^n(\underline{x}) \ \phi_i(\underline{y}) d\underline{y} \tag{2.7}$$

where $\langle \cdot, \cdot \rangle$ denotes the L^2 inner product over $\mathbb{R}^d$, i.e.,

$$\langle f, g \rangle = \int_{\mathbb{R}^d} f(\underline{r}) g(\underline{r}) d\underline{r} \ .$$

To derive (2.7) we have used the Galerkin method applied to an integrated form of (2.5). This is the same approach as that used by Bercovier & Pironneau (1982), Douglas & Russell (1982) and Pironneau (1982), for example.

A second, alternative, formulation was introduced by Benqué et al (1982), which is referred to here as the weak Lagrange-Galerkin method. It introduces new test functions $\psi_i(\cdot, t)$, which are not only different from the basis functions ϕ but depend on time. Multiplying (2.1) by this test function and integrating in space and time we get

$$\int_t^{t+\Delta t} \langle u_t + \underline{a} \cdot \underline{\nabla} u, \psi_i \rangle \, dt = 0 \ . \tag{2.8a}$$

Integrating by parts in both space and time, we obtain

$$\langle u(\cdot,t+\Delta t)\ ,\ \psi_i(\cdot,t+\Delta t)\rangle - \langle u(\cdot,t)\ ,\ \psi_i(\cdot,t)\rangle$$

$$= \int_t^{t+\Delta t} \langle u, \partial_t \psi_i + \underline{\nabla}\cdot(\underline{a}\ \psi_i)\rangle\ dt\ . \tag{2.8b}$$

Using the incompressibility condition, (2.2), $\underline{\nabla}\cdot(\underline{a}\psi_i)$ can be rewritten as $\underline{a}\cdot\underline{\nabla}\ \psi_i$ so that this last term vanishes if the test functions satisfy

$$\psi_i(\underline{X}(\cdot,t;t+\tau)\ ,\ t+\tau) = \psi_i(\cdot,t)\ . \tag{2.8c}$$

In order to solve (2.8c) a final condition is imposed on ψ_i by setting

$$\psi_i(\cdot,t+\Delta t) = \phi_i(\cdot)\ . \tag{2.8d}$$

Substituting the finite element approximation (2.6) into (2.8b) and using (2.8c) and (2.8d) gives

$$\langle U^{n+1}, \phi_i\rangle = \int U^n(\underline{x})\ \psi_i(\underline{x}, t^n)\ d\underline{x}\ :$$

or, equivalently,

$$\langle U^{n+1}, \phi_i\rangle = \int U^n(\underline{x})\ \phi_i(\underline{y})\ d\underline{x}\ . \tag{2.9}$$

Although (2.9) and (2.7) look very similar, and indeed are, we shall later use only the weak Lagrange-Galerkin method. This is preferred for a number of reasons. Firstly (2.9) ensures conservation even when the integral is approximated. This is not the case with the direct method. Furthermore the weak method deals more naturally with

source and boundary terms which will appear in integral form in (2.5b).

The EPIC algorithm is just a very specific approximation of the direct Lagrange-Galerkin method. Priestley (1986), Süli (1987), Morton, Priestley & Süli (1988) have shown that both the weak and direct versions are conditionally unstable for large classes of quadrature rules that integrate quadratics exactly when linear or quadratic basis functions are used. The EPIC algorithm works by using a compound trapezium rule to evaluate both the right-hand side integral and the mass-matrix. If the full mass-matrix were used the scheme would again become unstable but the use of the same compound trapezium rule on the left-hand side introduces just the right amount of mass-lumping to stabilize the scheme. As the number of sub-intervals is increased the amount of lumping is reduced. Conversely, if no sub-intervals are used, i.e. a vertex quadrature is used, then the mass-matrix becomes the identity matrix and we obtain the semi-Lagrangian method.

Perhaps the fact that the semi- or quasi-Lagrangian method performs so well is a tribute to the potential of the method, first described by Courant, Isaacson and Rees (1952). However, much better results can be obtained by the use of a Lagrange-Galerkin method. As a demonstration of the good properties of this method a Fourier analysis of both the semi-Lagrangian and exactly integrated Lagrange-Galerkin methods has been performed. Figure 1 shows, for various values of the CFL number υ , the square of the absolute value of the amplification factor, $|\lambda|^2$, against $\sin^2(\theta/2)$.

It is clear that much less damping occurs for all modes and CFL numbers for the Lagrange-Gakerkin method than for the semi-Lagrangian method. It should be noted that both schemes are unconditionally stable, i.e. $|\lambda|^2 \leq 1$. Of course this lack of damping is only a part of the story. We also need to consider the speed at which the modes are

propagated. If a mode were being propagated at entirely the wrong speed it would be better for that mode to be severely damped.

Now consider solutions to the differential equation

$$u_t + au_x = 0 \ . \tag{2.10}$$

of the form

$$u(x,t) = e^{i(\omega t - \xi x)} \ . \tag{2.11}$$

For every real wave number ξ we assume that there is a corresponding real value of the frequency ω such that (2.11) is a solution of (2.10). The relation $\omega = \omega(\xi)$ is called the dispersion relation for the differential equation. The phase speed is then

$$c(\xi) = \omega(\xi)/\xi \tag{2.12}$$

and the group velocity

$$C(\xi) = \frac{d\omega(\xi)}{d\xi} \ . \tag{2.13}$$

For the linear advection equation (2.10) we find, substituting in (2.11), that

$$c(\xi) = C(\xi) = a \ . \tag{2.14}$$

When using a numerical scheme (2.11) is replaced by

$$U_j^n = e^{i(\omega n\Delta t - \xi j\Delta x)} \ . \tag{2.15}$$

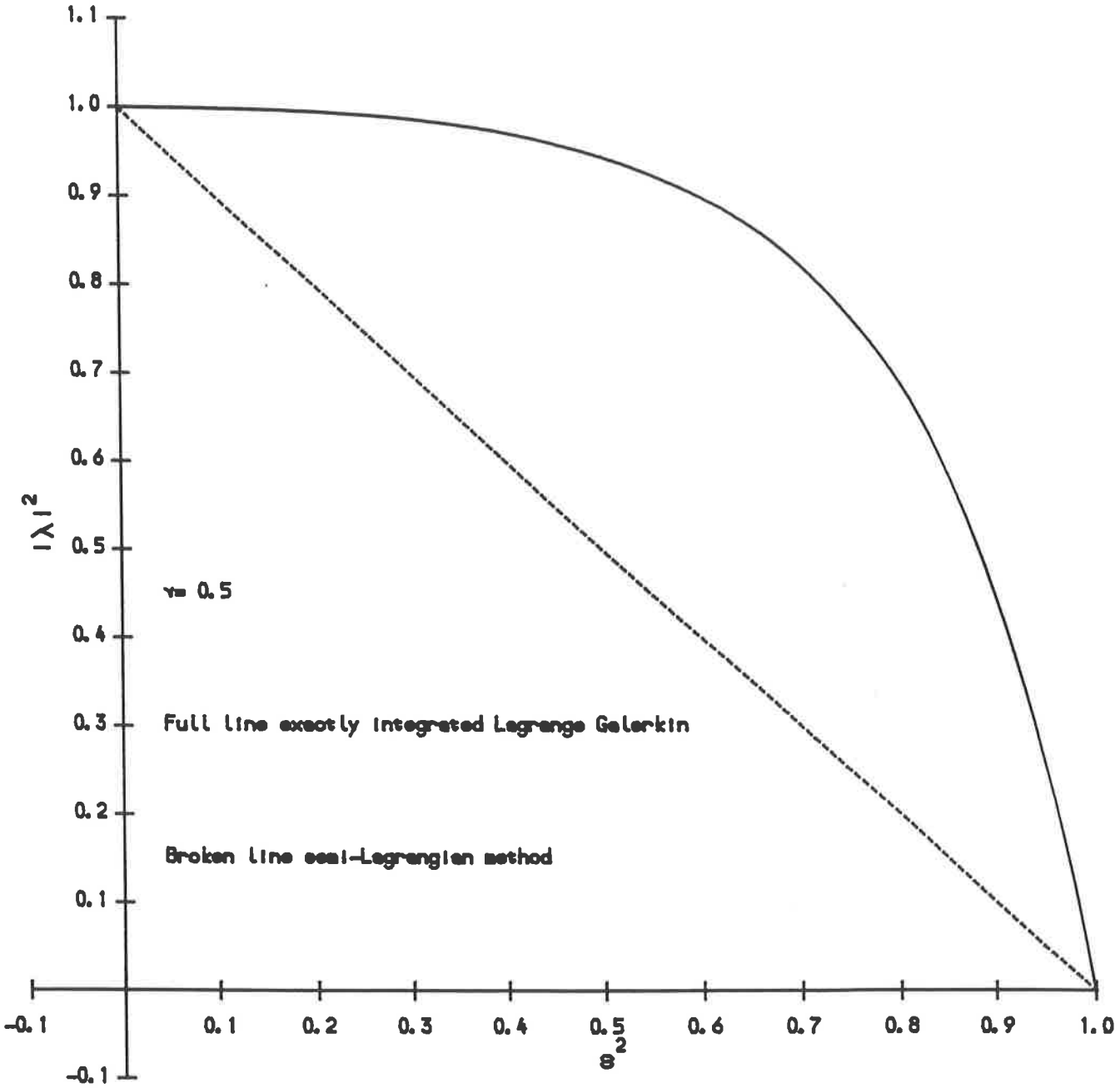
1.1
1.0
0.9
0.8
0.7
0.6
0.5
0.4
0.3
0.2
0.1
-0.1
$|\lambda|^2$
γ= 0.5
Full line exactly integrated Lagrange Galerkin
Broken line semi-Lagrangian method
0.1
0.2
0.3
0.4
0.5
0.6
0.7
0.8
0.9
1.0
s^2

Figure 1a

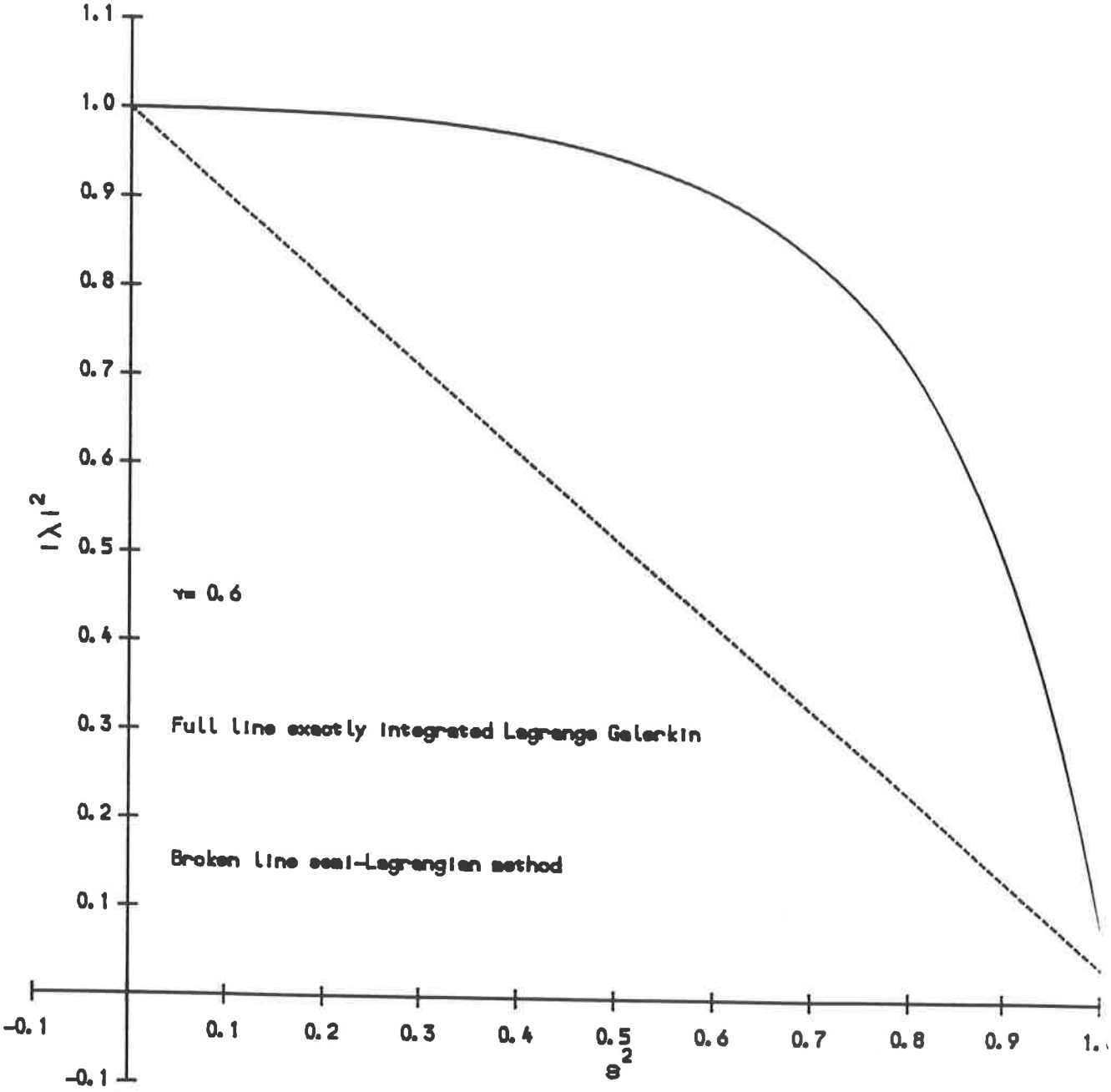
1.1
1.0
0.9
0.8
0.7
0.6
0.5
0.4
0.3
0.2
0.1
-0.1
-0.1
0.1
0.2
0.3
0.4
0.5
0.6
0.7
0.8
0.9
1.
$|\lambda|^2$
s^2
γ= 0.6
Full line exactly integrated Lagrange Galerkin
Broken line semi-Lagrangian method

Figure 1b

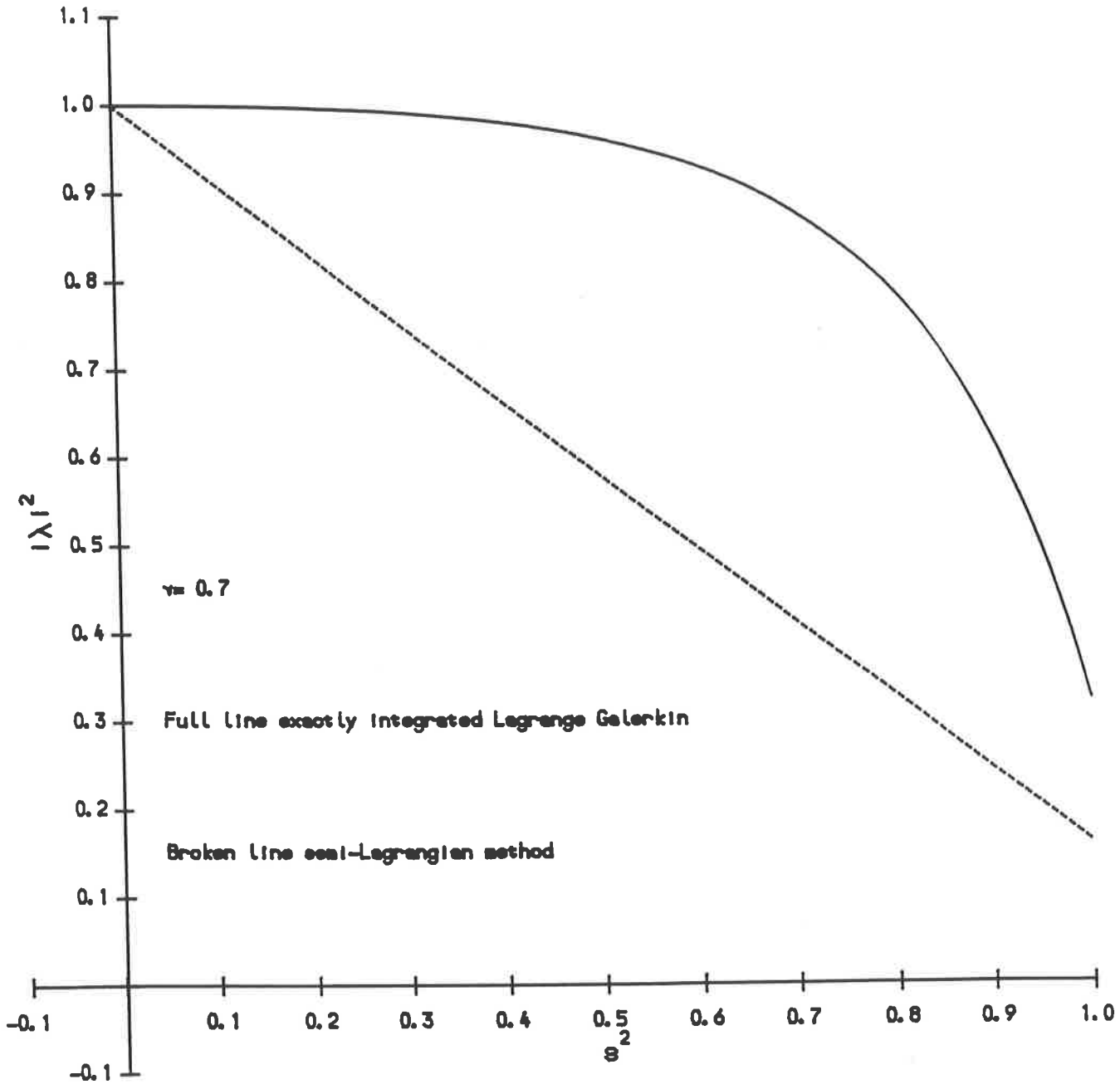
1.1
1.0
0.9
0.8
0.7
0.6
0.5
0.4
0.3
0.2
0.1
-0.1
$|\lambda|^2$
ν= 0.7
Full line exactly integrated Lagrange Galerkin
Broken line semi-Lagrangian method
-0.1
0.1
0.2
0.3
0.4
0.5
0.6
0.7
0.8
0.9
1.0
s^2

Figure 1c

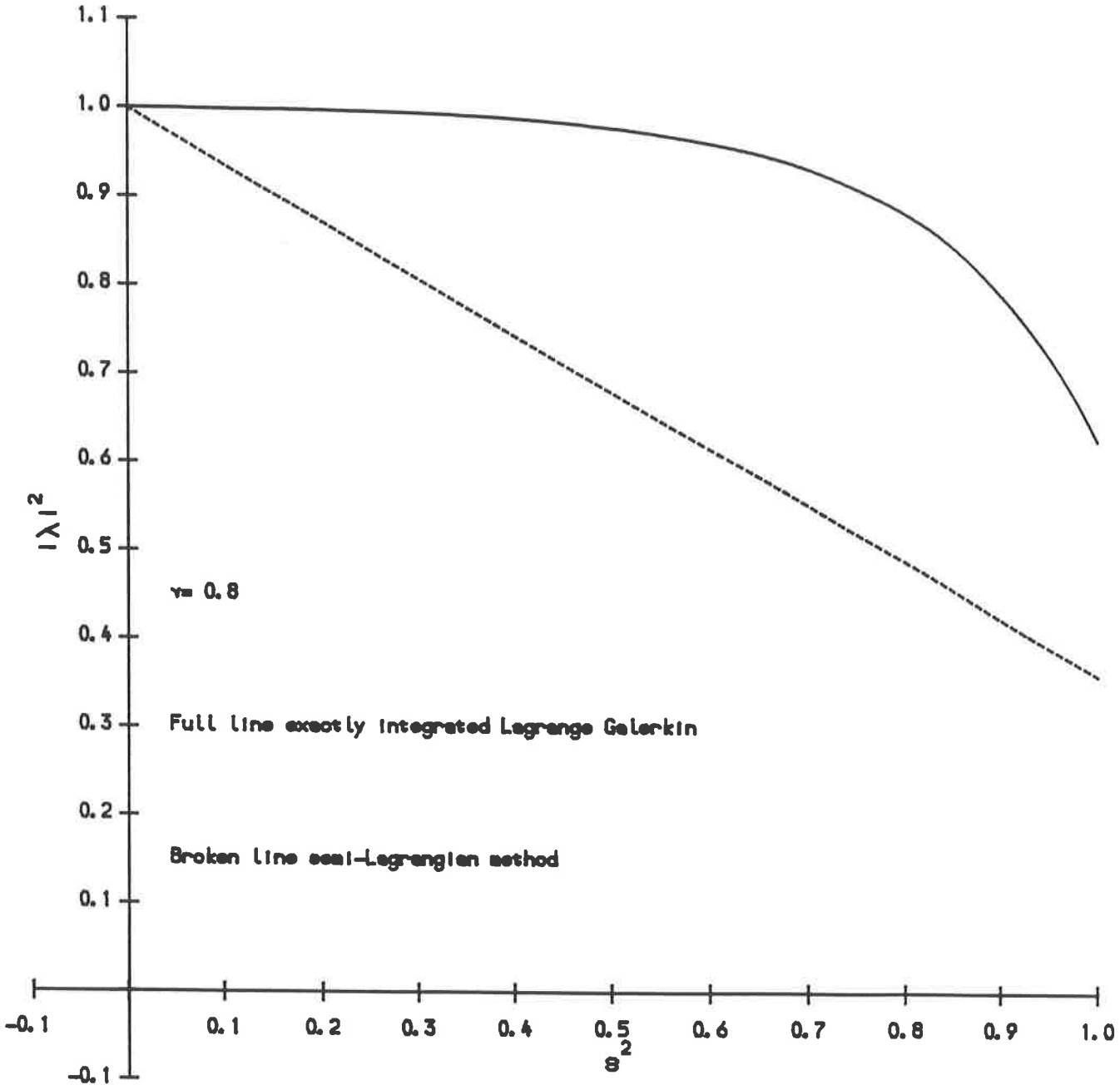
1.1
1.0
0.9
0.8
0.7
0.6
0.5
0.4
0.3
0.2
0.1
-0.1
$|\lambda|^2$
ν= 0.8
Full line exactly integrated Lagrange Galerkin
Broken line semi-Lagrangian method
-0.1
0.1
0.2
0.3
0.4
0.5
0.6
0.7
0.8
0.9
1.0
s^2

Figure 1d

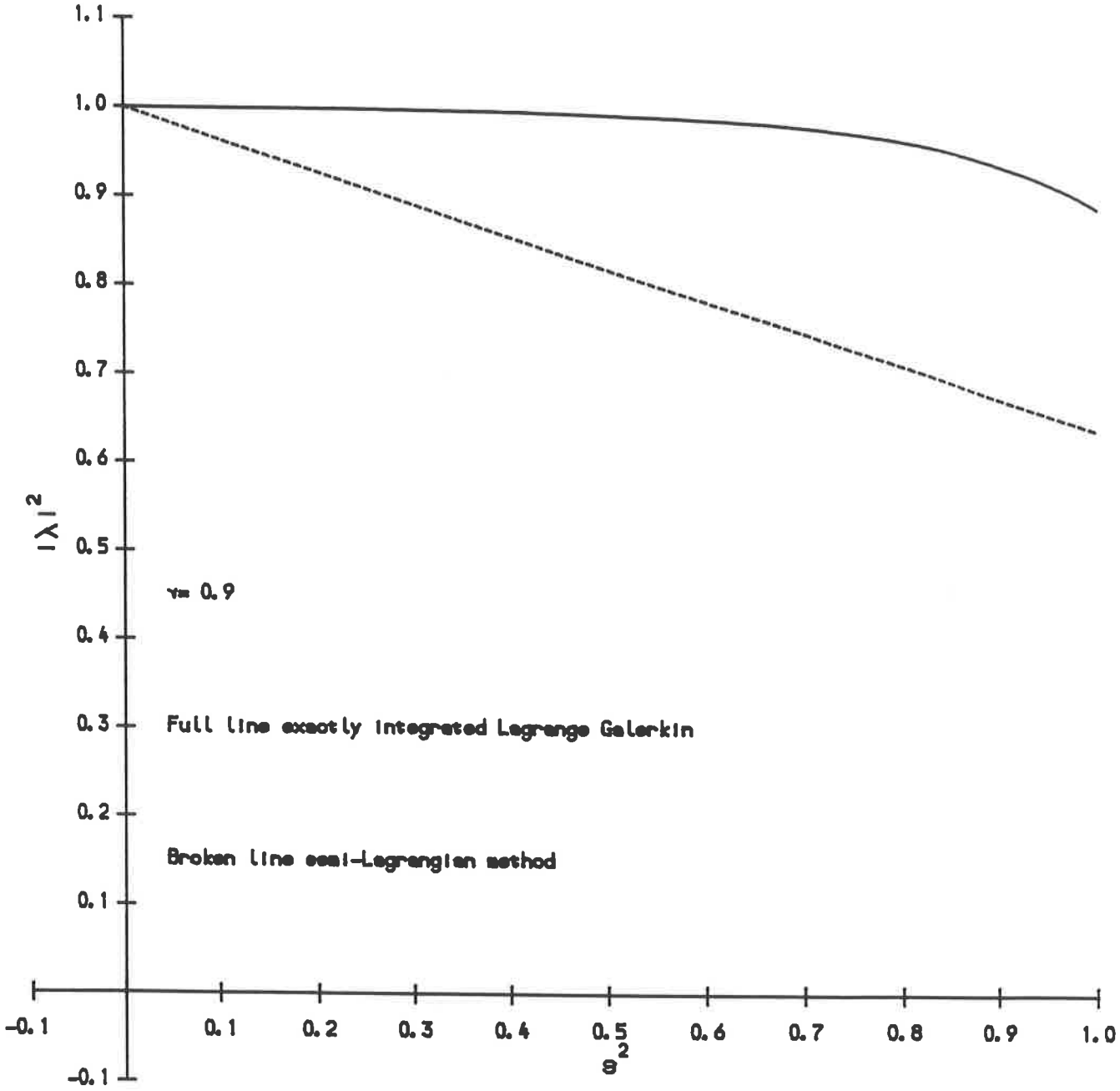
1.1
1.0
0.9
0.8
0.7
0.6
0.5
0.4
0.3
0.2
0.1
-0.1
$|\lambda|^2$
γ= 0.9
Full line exactly integrated Lagrange Galerkin
Broken line semi-Lagrangian method
-0.1
0.1
0.2
0.3
0.4
0.5
0.6
0.7
0.8
0.9
1.0
θ^2

Figure 1e

Substituting (2.15) into the difference equation produced by the semi-Lagrangian method (or, equivalently, the method of characteristics) produces

$$\omega_{s-L}(\xi) = \frac{\arcsin\left[\frac{a\Delta t}{\Delta t}\sin(\xi\Delta x)\right]}{\Delta t} \quad . \tag{2.16}$$

Dividing by ξ then produces the phase speed, $c_{s-L}(\xi)$ for the semi-Lagrangian method. This is more enlightening when it is expanded as a Taylor series to produce

$$c_{s-L}(\xi) = a + \frac{1}{6}(a^3\Delta t^3 - a\Delta x^2)\xi^2 + O(\xi^4) \quad . \tag{2.17}$$

Performing a similar calculation with the Lagrange-Galerkin method produces the dispersion relation

$$\omega_{s-L}(\xi) = \frac{\arcsin\left[\frac{a\Delta t(a^2\Delta t^2\cos(\xi\Delta x) - a^2\Delta t^2 + 3\Delta x^2)\sin(\xi\Delta x)}{\Delta x^3(2 + \cos(\xi\Delta x))}\right]}{\Delta t}$$

and again expanding $c_{L-G}(\xi)$ as a Taylor series we get

$$c_{L-G}(\xi) = a - \frac{a}{360}(3a^4\Delta t^4 - 5\Delta x^2a^2\Delta t^2 + 2\Delta x^4)\xi^4 + O(\xi^6) \quad . \tag{2.18}$$

Comparing (2.18) and (2.17) we see that the Lagrange-Galerkin method produces a phase speed two orders of magnitude more accurate.

It is therefore seen that the Lagrange-Galerkin scheme not only produces much less damping of waves but also transports them with a much more accurate speed. This comparison is, perhaps, a little unfair on

the semi-Lagrangian method because its practitioners generally prefer a cubic-interpolation which produces much better results than with the linear interpolation. However, if we used cubic elements in the Lagrange-Galerkin approach similar results would follow.

3. SPECTRAL LAGRANGE-GALERKIN

3.1 The Implementation

It has been shown that the Lagrange-Galerkin method with linear elements is a much more attractive proposition than the semi-Lagrangian method, even though the latter has already proved its worth in the meteorological literature.

However, the application of the Lagrange-Galerkin method is not a straightforward matter due to the conditional instability introduced by quadrature, see Priestley (1986), Morton, Priestley & Süli (1988). Quadrature is needed in all but the most trivial cases. The EPIC algorithm of Eastwood & Arter (1986) performs a stable quadrature but is expensive. Priestley et al (1986,1988) proposed a different technique that was stable and efficient on rectangular elements but again becomes expensive if a distorted rectangular mesh or a triangular mesh is required.

The analysis of Priestley (1986) restricted itself to the traditional finite element basis functions of piecewise linear, piecewise quadratic etc.. However, Süli (1988b) noted that if global basis functions were used, as in spectral methods, then the method would again become stable. This was later formalized in Süli and Ware (1988) where it is shown that, for an n mode approximation, the only condition placed upon the compound trapezium rule used as a quadrature is that at least $n+1$ points are used.

A further benefit of using orthogonal polynomials is the fact that, given suitable normalization factors

$$\int_{\Omega} s_m(x)s_n(x)dx = \begin{cases} 1 & \text{if } m = n \\ 0 & \text{if } m \neq n \end{cases}$$

which means that the mass matrix reduces to the identity matrix resulting in a major saving in computer time for the method.

The co-ordinate system that is used in the meteorological content used is normally (λ,μ) where $\mu = \sin\theta$. Here λ is the longitude and θ is the latitude with

$$0 \leq \lambda \leq 2\pi$$

and

$$-1 \leq \mu \leq 1 .$$

The appropriate orthogonal basis functions are

$$Y_{m,n}(\mu,\lambda) = P_{m,n}(\mu)e^{im\lambda}$$

where $P_{m,n}(\mu)$ denotes the associated Legendre function of the first kind given by

$$P_{m,n}(\mu) = \left[\frac{(2n+1)(n-m)!}{(n+m)!}\right]^{\frac{1}{2}} \frac{(1-\mu^2)^{m/2}}{2^n n!} \frac{d^{n+m}}{d\mu^{n+m}} (\mu^2-1)^n .$$

The basis functions satisfy the orthogonality relation

$$\frac{1}{4\pi} \int_0^{2\pi} \int_{-1}^{1} Y_{m,n} Y^*_{m',n'} \, d\mu d\lambda = \begin{cases} 1 & \text{for } (m',n') = (m,n) \\ 0 & \text{for } (m',n') \neq (m,n) . \end{cases}$$

Here we have used Y^* to denote the complex conjugate of Y .

Denoting the radius of the earth by a we expand any function ψ on the surface of the globe in terms of these spherical harmonics as

$$\psi(\mu,\lambda,t) = a^2 \sum_{m=-M}^{M} \sum_{n=|m|}^{|m|+J} \psi_{m,n}(t)\, Y_{m,n}(\mu,\lambda) \quad . \tag{3.1}$$

(Here J may be a function of m and defines the type of truncation to be made. In rhomboidal truncation $J = M$, whilst with triangular truncation $J = M - |m|$.

The coefficients $\psi_{m,n}$ can be obtained from the inverse transform formula

$$\psi_{m,n}(t) = \frac{1}{4\pi a^2} \int_0^{2\pi} \int_{-1}^{1} \psi(\mu,\lambda,t) Y^*_{m,n} d\mu d\lambda \quad . \tag{3.2}$$

Since $\psi(\mu,\lambda,t)$ must be real $\psi_{m,n}$ must satisfy

$$\psi_{-m,n} = (-1)^m \psi^*_{m,n}$$

which is implied by the use of the relation

$$P_{-m,n} = (-1)^m P_{m,n} \quad .$$

That describes the horizontal discretization and it remains to look at the vertical discretization. In order to achieve compatability with current meteorological codes a finite difference approach has been used

in the vertical. In essence this means that a two-dimensional problem is solved on each horizontal layer. A cubic interpolation is performed between layers when necessary. Another way of looking at the use of finite differences in the vertical to regard it as arising from the use of cubic finite elements in the vertical together with vertex quadrature - a procedure that we have already castigated! For the time being though we will persevere with this approach but in the final section alternatives will be discussed.

The other major difficulty with the vertical direction is the nature of the co-ordinates in that direction. Owing to difficulties caused by orography the straightforward z = height co-ordinate is not used.

Following Simmons & Burridge (1981) the vertical co-ordinate, η, is a monotonic function of pressure p and is dependent on the surface pressure p_o :

$$\eta = h(p,p_o) \ ,$$

where $h(0,p_o) = 0$ and $h(p_o,p_o) = 1$. Here we shall use the hybrid vertical co-ordinates defined by

$$\eta_{k+\frac{1}{2}} = \frac{A_{k+\frac{1}{2}}}{p_o} + B_{k+\frac{1}{2}} \ .$$

The values of A,B and p_o are tabulated in the Appendix.

The weak Lagrange-Galerkin method is now

$$U_{m',n',\eta'}(t+\Delta t) = \sum_{\eta=0}^{\text{vertical levels}} \frac{1}{4\pi a^2(z')} \int_0^{2\pi} \int_{-1}^{1} a^2(z) \sum_{m=-M}^{M} \sum_{n=|m|}^{|m|+J} U_{m,n,\eta}\, Y_{m,n}(\mu,\lambda)$$

$$\cdot Y^*_{m',n'}(\vec{\mu},\vec{\lambda})\, d\mu\, d\lambda \ . \qquad (3.3)$$

In (3.3) $(\vec{\mu},\vec{\lambda},\eta')$ denotes the transported position of a particle that was at (μ,λ,η). Of course η' has to take on integer values and so by $U_{m',n',\eta'} = I$ we implicitly assume that a cubic interpolation has already been performed.

Another snag with the vertical co-ordinate is the fact that in the scheme we require $a^2(z)$. Theoretically z can be recovered from known information but this is by no means a straightforward procedure and we would rather avoid such a calculation if possible. Fortunately, because of the large radius of the earth (approximately 6400km) and because of the relatively thin nature of the atmosphere (approximately 20km), $a^2(z) \simeq a^2(z')$ and so we can replace (3.3) by

$$U_{m',n',\eta'}(t+\Delta t) = \frac{1}{4\pi} \sum_{\eta=0}^{\text{vertical levels}} \int_{0}^{2\pi} \int_{-1}^{1} \sum_{m=-M}^{M} \sum_{n=|m|}^{|m|+J} U_{m',n',\eta} Y_{m,n}(\mu,\lambda)$$

$$Y^{*}_{m',n'}(\vec{\mu},\vec{\lambda})\, d\mu\, d\lambda \,. \qquad (3.4)$$

3.2 The Test Problem

Before embarking on the real problem of interest, that of the distribution of a passive chemical agent in the atmosphere (which will be described in a later report), a rather simpler problem is attempted here for which there is an analytic solution. This involves the rotation of a cone around a sphere under a constant velocity field and follows the paper of Ritchie (1987), from which the equations in this section have been reproduced for convenience.

Using longitude-latitude, (λ,θ), coordinates the two-dimensional advection equation can be written as

$$\frac{\partial F}{\partial t} + \frac{u}{a \cos\theta} \frac{\partial F}{\partial \lambda} + \frac{v}{a} \frac{\partial F}{\partial \theta} = 0 \qquad (3.5)$$

where a is the radius of the earth, u is the zonal wind component and v is the meridional wind component.

If we consider rotation with a constant angular velicity ω about an axis passing through the centre of the earth and through some point P' on the earth's surface with coordinates (λ_o, θ_o) in the (λ, θ) system, we can define another coordinate system (λ', θ') that has the point P' as its north pole. Various useful identities that can be derived from spherical trigonometry relating the two coordinate systems are

$$\sin \theta' = \sin \theta \sin \theta_o + \cos \theta \cos \theta_o \cos(\lambda - \lambda_o) \tag{3.6a}$$

$$\sin \theta = \sin \theta' \sin \theta_o - \cos \theta' \cos \theta_o \cos \lambda' \tag{3.6b}$$

$$\cos \theta' \sin \lambda' = \cos \theta \sin(\lambda - \lambda_o) \ . \tag{3.6c}$$

In the (λ', θ') system we require

$$\frac{\partial \lambda'}{dt} = \omega$$

$$\frac{\partial \theta'}{dt} = 0 \ .$$

This can be achieved by defining

$$u = a\omega[\cos \theta \sin \theta_o - \cos(\lambda - \lambda_o) \sin \theta \cos \theta_o] \tag{3.7a}$$

$$v = a\omega \sin (\lambda - \lambda_o) \cos \theta_o \ . \tag{3.7b}$$

Using the relations

$$u = a \cos \theta \frac{\partial \lambda}{dt}$$

and

$$v = a \frac{\partial \theta}{dt}$$

we return to velocities in the (λ,θ) system. In the present case we use a (λ,μ) system where $\mu = \sin\theta$, so that the velocity is

$$\frac{\partial \mu}{dt} = \cos\theta \frac{\partial \theta}{dt} .$$

In the (λ',θ') system (3.5) becomes

$$\frac{\partial F'}{dt} + \omega \frac{\partial F'}{d\lambda'} = 0 \qquad (3.8)$$

which has the solution

$$F'(\lambda',\theta',t) = f'(\lambda' - \omega t,\theta') \qquad (3.9)$$

where f' is calculated from the initial conditions in the (λ',θ') system. Using the equations (3.6) we can derive

$$\lambda'(\lambda,\theta) = \tan^{-1}\left\{\frac{\sin(\lambda-\lambda_o)}{[\sin\theta_o \cos(\lambda-\lambda_o) - \cos\theta_o \tan\theta]}\right\}$$

$$\theta'(\lambda,\theta) = \sin^{-1}\{\sin\theta \sin\theta_o + \cos\theta \cos\theta_o \cos(\lambda-\lambda_o)\}$$

and so, from an initial profile $f'(\lambda',\theta')$ in the (λ',θ') coordinate system, the exact solution in the (λ,θ) system is given by

$$F(\lambda,\theta,t) = f'(\lambda'(\lambda,\theta) - \omega t \ , \ \theta'(\lambda,\theta)) \ . \qquad (3.10)$$

The initial data chosen was

$$f(\lambda,\theta) = 100e^{-\pi^2 r^2/L^2} \tag{3.11}$$

where L^2 is just a positive constant and

$$r^2 = (\lambda - \lambda_F)^2 + (\theta - \theta_F)^2 \ . \tag{3.12}$$

(λ_F,θ_F) are the chosen coordinates for the centre of the Gaussian hill.

A significant problem with Lagrangian methods on spheres is that of the accurate calculation of the trajectories at the two poles. Using straightline approximations in (λ,μ) space, i.e.

$$\vec{\lambda} = \lambda + \Delta t\dot{\lambda}$$
$$\vec{\mu} = \mu + \Delta t\dot{\mu}$$

leads to very poor results, particularly near the poles. Straightline trajectories are quite good in Cartesian geometries and so, following Ritchie (1987) the procedure for calculating trajectories is performed in the iterative manner,

$$\underline{r}_{k+1} = b_k(\underline{g} + \Delta t\dot{\underline{r}}_k) \ , \tag{3.13}$$

where $\underline{g}$ is the starting point and $\underline{r}_{k+1}$ is the latest prediction for the end point of the trajectory. If $\underline{g}$ lies on the earth's surface, i.e. $|\underline{g}| = a$, then when solving in Cartesian space the factor b_k must be introduced in order to ensure that $|\underline{r}_k| = a \ \forall k$.

If the longitude and latitude of the grid point g are given by (λ_i, θ_j) the Cartesian coordiantes of g are given by

$$X_G = \cos \lambda_i \cos \theta_j$$
$$Y_G = \sin \lambda_i \cos \theta_j$$
$$Z_G = \sin \theta_j \ .$$

Given that $\underline{r}_k = (\lambda_k, \theta_k)$ we can find the normalized velocities

$$\tilde{u}_k = u(\lambda_k, \theta_k, t)/a$$
$$\tilde{v}_k = v(\lambda_k, \theta_k, t)/a$$

and then the normalized Cartesian velocity components are

$$\dot{X}_k = - \tilde{u}_k \sin \lambda_k - \tilde{v}_k \cos \lambda_k \sin \theta_k$$
$$\dot{Y}_k = \tilde{u}_k \cos \lambda_k - \tilde{v}_k \sin \lambda_k \sin \theta_k$$
$$\dot{Z}_k = \tilde{v}_k \cos \theta_k \ .$$

The required value of b_k can now be written as

$$b_k = \{1 + \Delta t^2(\dot{X}_k^2 + \dot{Y}_k^2 + \dot{Z}_k^2) - 2\Delta t(\dot{X}_k X_G + \dot{Y}_k Y_G + \dot{Z}_k Z_G)\} \ .$$

Equation (3.13) then becomes

$$X_{k+1} = b_k(X_G + \Delta t\dot{X}_k)$$
$$Y_{k+1} = b_k(Y_G + \Delta t\dot{Y}_k)$$
$$Z_{k+1} = b_k(Z_G + \Delta t\dot{Z}_k) \ .$$

The iteration is finally completed by calculating

$$\lambda_{k+1} = \tan^{-1}(Y_{K+1}/X_{k+1})$$
$$\theta_{k+1} = \sin^{-1}(Z_{K+1})$$
$$\mu_{k+1} = Z_{K+1} \ .$$

4. RESULTS

4.1. The 2-D Rotating Cone Problem

We now choose the following parameters to be:-

$$(\lambda_o, \theta_o) = (\pi, \pi/4)$$
$$(\lambda_F, \theta_F) = (\pi, -\pi/4)$$
$$L = 1/2$$
$$\omega = 3.6E - 6 \ .$$

This value of ω implies that a complete rotation will occur in approximately 20 days. The initial data is shown in Figure 2. The surface plots of the solution are not particularly illuminating and so the results are just presented in tabular form.

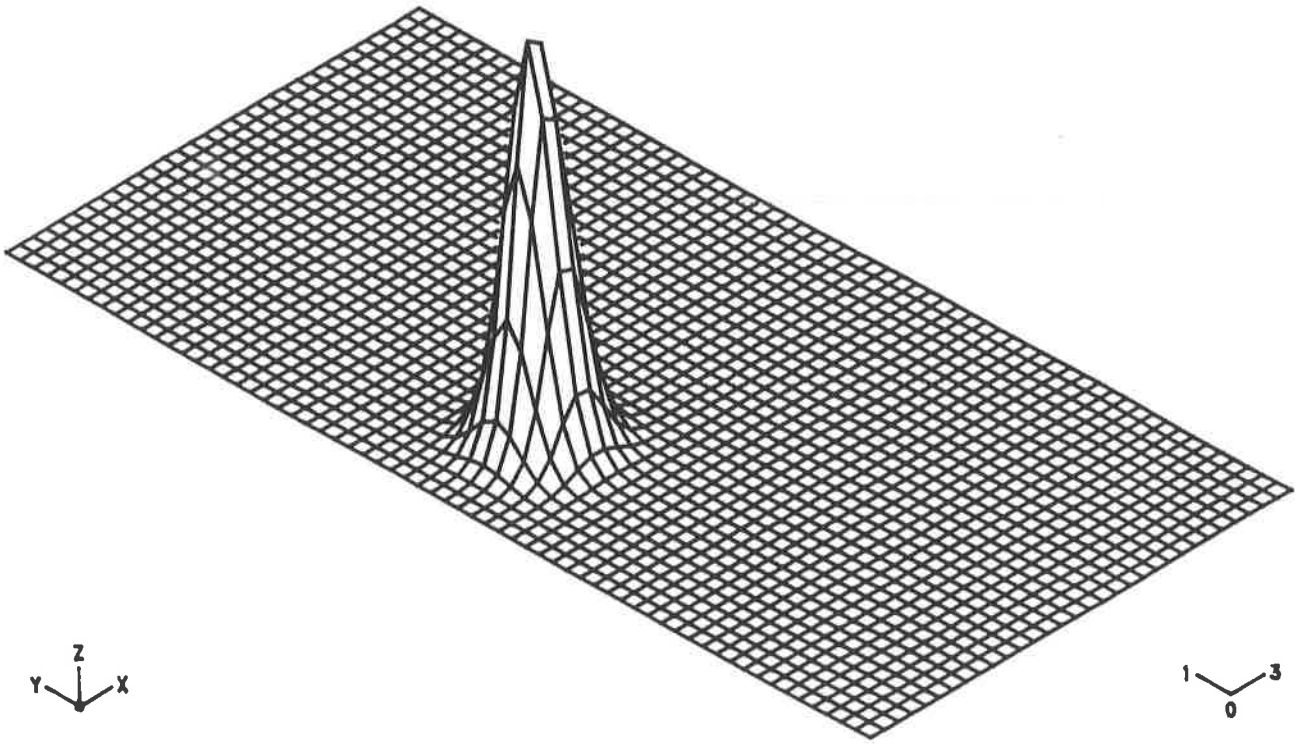

Figure 2

First a few comments about the results. The minimum and maximum values are really superfluous and it is the error we should really look at. However, it is natural to look at such obvious indicators of accuracy as extreme values, and indeed for quantities such as humidity negative values are meaningless and values greater than 100%, caused by overshoot, can lead to unwarranted predictions of precipitation. It is desirable, therefore, to have a method that can advect data with minimal overshoot and undershoot. The initial data is taken pointwise which means that at time zero the minimum is 0 and the maximum, because it does not fall on a grid point, is not 100 but 97.45. This can be misleading because, if a projection of the initial data onto spectral space is done, then the minimum and maximum become - 0.8 and 95 . More importantly the error is calculated as 0.817. These figures should be borne in mind when looking at the tables. These projection errors are for the T21 spectral model (triangular truncation with 21 modes) and will obviously be reduced as the resolution of the model is increased. The errors given are in the discrete ℓ_2 norm. The continuous L_2 norm is defined as

$$||\text{error}||_2 = \left[\frac{1}{4\pi}\int_0^{2\pi}\int_{-1}^{1} (\text{exact solution} - \text{approx. solution})^2 \, d\lambda \, d\mu\right]^{\frac{1}{2}} . \tag{4.1}$$

The discrete ℓ_2 norm is the same except that the integrals in (4.1) are replaced by quadratures.

There are three sources of error in the Lagrange-Galerkin method. First there is a projection error in the exactly integrated method. Secondly, in practical problems where we have to use quadrature there is

the added error because we are only performing the projection approximately. Thirdly, there will be errors in the calculation of the trajectories. Given the spectral model there is not much we can do about the first source of error. The quadrature is something that we can control as is the calculation of the trajectories. One way, then, of reducing the error in the calculation of the trajectories is to reduce the time-step. However, this then means that we will do more projections and so increase this source of error. From the tables, though, we see that the trajectory error dominates the projection error. Table 1 gives values for the trajectories calculated as straight-lines in (λ,μ) space and Table 2 gives the results from calculating the paths in Cartesian space.

Number of time-steps	Minimum	Maximum	ℓ_2 error
40	-0.9259	72.45	5.740
48	-0.8806	75.68	4.835
60	-0.8418	78.95	3.946
80	-0.8093	82.25	3.081
96	-0.8017	83.89	2.664
120	-0.7949	85.47	2.271
160	-0.8103	86.89	1.921
192	-0.8261	87.47	1.779
240	-0.8468	87.88	1.679

Table 1: Trajectories calculated in (λ,μ) space.

Number of time-steps	Minimum	Maximum	ℓ_2 error
40	-0.6616	57.44	9.405
48	-0.6742	63.04	7.926
60	-0.6523	68.88	6.385
80	-0.6775	74.64	4.890
96	-0.6948	77.54	4.155
120	-0.7358	80.37	3.451
160	-0.7863	83.05	2.797
192	-0.8139	84.27	2.500
240	-0.8403	85.32	2.240

Table 2: Trajectories calculated in Cartesian space

We see that neither approach suffers from undershoot to any significant degree and, although both suffer from some degradation of the peak, we see that if the time-steps are small enough the peak is maintained very well. Both methods have a pleasing reduction in ℓ_2 error but again these figures are better when we solve for the trajectories in spherical space rather than Cartesian space. The results using Cartesian space perform particularly badly when very large time-steps are used. It should be noted, though, that the solving of the trajectories in Cartesian space is particularly recommended for the problems caused by the poles. In this problem the cone did not traverse either pole.

We now consider the effect on the solution caused by crossing a pole. All parameters are the same except that we choose

$$(\lambda_F, \theta_F) = (\pi, 0) \ .$$

This ensures that the cone will pass directly over the North Pole after half a revolution. It is worth pointing out that any undue under/overshoot is not a result of instability but is just due to errors incurred in travelling over the pole. The initial projection errors result in a minimum of -0.0255, a maximum of 95.347 and an ℓ_2 error of 0.0589. The initial data can be seen in Figure 3. Tables 3 and 4 correspond to Tables 1 and 2 for the new initial data.

Number of time-steps	Minimum	Maximum	ℓ_2 error
40	-84.65	219.8	51.72
48	-89.59	239.2	54.84
60	-82.84	246.9	53.54
80	-53.22	226.9	44.36
96	-36.24	210.7	38.49
120	-29.09	194.5	33.02
160	-19.92	167.8	24.43
192	-15.41	153.6	19.86
240	-11.26	139.3	15.35

Table 3: Trajectories calculated in (λ,μ) space.

Number of time-steps	Minimum	Maximum	ℓ_2 error
40	-1.18	147.6	31.08
48	-6.17	137.2	26.49
60	-4.87	118.2	20.79
80	-2.99	96.60	16.02
96	-0.92	94.72	13.91
120	-0.73	100.4	10.66
160	-1.32	97.73	10.21
192	-1.76	106.6	7.37
240	-1.45	105.6	6.01

Table 4: Trajectories calculated in Cartesian Space.

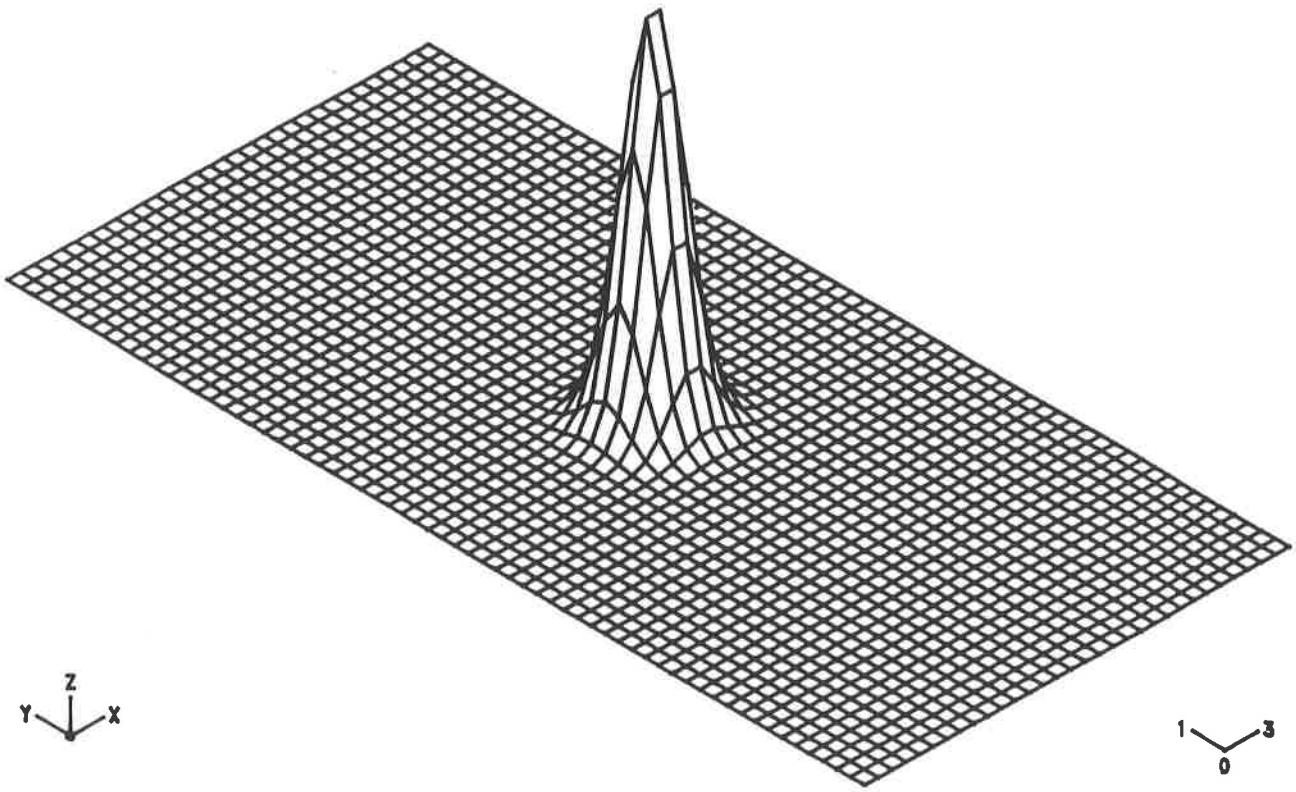

Figure 3

We see here, with some satisfaction, that calculating the trajectories in Cartesian space has performed much better than calculating them directly in the spherical geometry. Although both sets of results are converging, at no point do the results in Table 3 become adequate. Tables 3 and 4 reinforce the comments made earlier about the need for the accurate calculation of the trajectories.

We now consider the effects of improving the solution of the trajectories. A Runge-Kutta technique might be more efficient but for the sake of simplicity a compound Euler method was used to give the results in Table 5. All trajectories are calculated in Cartesian space and the problem is the same as for that to which Tables 3 and 4 refer.

Number of time-steps	Minimum	Maximum	ℓ_2 error
40	-0.617	85.64	5.135
48	-2.142	77.39	7.969
60	-0.885	79.52	5.362
80	-1.425	83.65	4.765
96	-1.462	94.29	3.430
120	-1.308	95.27	2.115
160	-0.979	93.76	1.594
192	-0.792	92.85	1.375
240	-0.599	91.78	1.202

Table 5: Accurate Cartesian Trajectories.

Here we see much more satisfactory results. There is a steady convergence, aside from the first result, although all the results give adequate answers. With a more accurate trajectory solver one might well hope that the 12hr. time-stepping would give results comparable to the 2 hour time-stepping.

The one question remaining is the size of the error that is made due to using an approximate projection, i.e. using quadrature of the integrals. In the periodic direction, for stability, we need only to use a maximum of M+1 quadrature points. We have been using (3M+1), i.e. 64, points. This is needed in the spectral model to deal with aliasing errors caused by non-linear terms. This is not a problem for us with this equation and so we can reduce the order of our quadrature. In Table 6 we present results obtained by using just 32 points in the periodic direction. Everthing else is the same as for the results in Table 5.

Number of time-steps	Minimum	Maximum	ℓ_2 error
40	-1.09	85.8	3.76
48	-3.26	81.44	8.68
60	-1.93	75.47	6.35
80	-2.05	77.84	5.59
96	-2.22	93.11	3.23
120	-1.36	93.07	2.13
160	-1.41	91.83	1.76
192	-1.41	91.15	1.62
240	-1.41	90.39	1.51

Table 6: Reduced order quadrature. (32 x 32)

Comparing these figures with those in Table 5 we see that there is not a great deal of difference. The errors in Table 5 are uniformly lower, with the exception of the first, but one might well ask if this marginal decrease in error was justified by a doubling of computer time.

5. CONCLUSIONS

We have shown that the spectral Lagrange-Galerkin method is a very formidable scheme for solving advection dominated problems on a sphere even on the extremely coarse meshes used here and is, arguably, a considerable improvement over the semi-Lagrangian method currently being used.

There is a considerable amount of further work to be done. The question of producing accurate, cheap, approximations to the trajectories needs to be resolved. It is hoped that soon this method will be tried on a full 3-D model of the atmosphere to predict the advection of a passive pollutant.

We mentioned earlier the mismatch between the representations in the horizontal and the vertical, spectral and finite difference. Since the code produced needs to be compatable with the current numerical weather prediction models this situation is likely to have to continue. However, a more pleasing approach would be to use a spectral method in the vertical also, see Machenhauer and Daley (1972).

APPENDIX

Parameters of 19-level hybrid vertical co-ordinate system. A and p_o are given in Pascals.

k	$A_{k+½}$	$B_{k+½}$
0	0.0	0.0
1	0.2E+4	0.0
2	0.4E+4	0.0
3	0.604611E+4	0.338993E-3
4	0.826793E+4	0.335719E-2
5	0.106095E+5	0.130700E-1
6	0.128511E+5	0.340771E-1
7	0.146985R+5	0.706498E-1
8	0.1586611E+5	0.125917
9	0.161162E+5	0.201195
10	0.153569E+5	0.295520
11	0.136215E+5	0.405409
12	0.111016E+5	0.524932
13	0.812714E+4	0.646108
14	0.512514E+4	0.759698
15	0.254987E+4	0.856438
16	0.783195E+3	0.928747
17	0.0	0.972985
18	0.0	0.992281
19	0.0	1.0

$$p_o = 0.101325E+6$$

6. REFERENCES

1. Bates, J.R., 1985, "Semi-Lagrangian advective schemes and their use in meteorological modelling." Lectures in Applied Mathematics. Vol. 22, pp. 1-29.

2. Benqué, J.P., Labadie, G. & Ronat, J., 1982, "A new finite element method for the Navier-Stokes equations coupled with a temperature equation." Proc. 4th Int. Symp. on Finite Element Methods in Flow Problems (Ed. T. Kawai), North-Holland, Amsterdam, Oxford, New York, pp. 295-301.

3. Bercovier, M. & Pironneau, O., 1982, "Characteristics and the Finite Element Method." Proc 4th Int. Symp. on Finite Element Methods in Flow Problems (Ed. T. Kawai), North-Holland, Amsterdam, Oxford, New York, pp. 67-73.

4. Courant, R., Isaacson, E., Rees, M., 1952, "On the solution of nonlinear hyperbolic differential equations by finite differences." Comm. Pure & Appl. Maths., Vol. V, 243-255.

5. Douglas, J. & Russell, T.F., 1982, "Numerical methods for convection-dominated diffusion problems based on combining the method of characteristics with finite element or finite difference procedures." SIAM J. Numer. Anal., 19, pp. 871-885.

6. Eastwood, J.W., & Arter, W., 1986, "EPIC-Beyond the ultimate difference scheme." Numerical Methods for Fluid Dynamics II (Ed. K.W. Morton, M.J. Baines), O.U.P., Oxford.

7. Lesaint, P., 1977, "Numerical solution of the equation of continuity." Topics in Numerical Analysis III (Ed. J.J.H. Miller), Academic Press, London, New York, San Francisco, pp. 199-222.

8. Machenhauer, B. & Daley, R., 1972, "A Baroclinic primitive equation model with a spectral representation in three dimensions." Report no. 4. Institut for Teoretisk Meteorologi, Kϕbenhauns Universitet.

9. Morton, K.W., & Priestley, A., 1986, "On characteristic and Lagrange-Galerkin methods." Pitman Research Notes in Mathematics Series (Ed. D.F. Griffiths & G.A. Watson), Longman Scientific and Technical, Harlow.

10. Morton, K.W., Priestley, A. & Süli, E., 1988, "Stability of the Lagrange-Galerkin method with non-exact integration", M^2AN, Vol. 22, no. 4. pp. 625-653.

11. Pironneau, O., 1982, "On the transport diffusion algorithm and its application to the Navier-Stokes equations." Numer. Math., 38, pp. 309-332.

12. Priestley, A., 1986, "Lagrange and characteristic Galerkin methods for evolutionary problems." D.Phil. Thesis, University of Oxford.

13. Ritchie, H., 1987, "Semi-Lagrangian advection on a Gaussian grid." Mon. Wea. Rev., 115, 608-619.

14. Robert, A.J. 1981, "A stable numerical integration scheme for the primitive meteorological equations." Atmos-Ocean, 19, 35-46.

15. Robert, A.J., 1982, "A semi-Lagrangian and semi-implicit numerical integration scheme for the primitive meteorological equations." J. Met. Soc. Japan, 60, 319-325.

16. Russell, T.F., 1980, "Time-stepping along characteristics with incomplete iteration for a Galerkin approximation of miscible displacement in porous media. "Ph.D. Thesis, University of Chicago.

17. Simmons, A.J. & Burridge, D.M., 1981, "An energy and angular-Momentum conserving vertical finite-difference scheme and hybrid vertical coordinates", Mon. Wea. Rev., 109, pp. 758-766.

18. Staniforth, A. & Temperton, C., 1986, "Semi-implicit semi-Lagrangian integration schemes for a baratropic finite-element regional model. "Mon. Wea. Rev., 114, 2078-2090/

19. Süli, E., 1987, "Stability and convergence of the Lagrange-Galerkin method with non-exact integration." The Mathematics of Finite Elements and Applications VI, MAFELAP 1987, (Ed. J.R. Whiteman), Academic Press.

20. Süli, E.E., 1988, "Convergence and nonlinear stability of the Lagrange-Galerkin method for the Navier-Stokes equations. "Numer. Math., 53, pp. 459-483.

21. Süli, E., 1988b, Private Communication.

22. Süli, E. & Ware, A., 1988, "A spectral method of characteristics for first-order hyperbolic equations". Oxford University Computing Laboratory, Numerical Analysis Report.

23. Temperton, C., & Ritchie, H., 1987, "Three-time-level semi-Lagrangian schemes in finite element and spectral models." Techniques for horizontal discretization in numerical weather prediction models, ECMWF Workshop Proceedings 2-4 November 1987.

AP/89:sd